Intensity noise-driven nonlinear fiber polarization scrambler

Massimiliano Guasoni,[1,*] Julien Fatome,[1] and Stefan Wabnitz[2]

[1]*Laboratoire Interdisciplinaire Carnot de Bourgogne, UMR 6303 CNRS-Université de Bourgogne, Dijon, France*

[2]*Dipartimento di Ingegneria dell'Informazione, Università degli Studi di Brescia, via Branze 38, Brescia 25123, Italy*

**Corresponding author: massimiliano.guasoni@u-bourgogne.fr*

Received May 7, 2014; revised June 25, 2014; accepted August 1, 2014;
posted August 4, 2014 (Doc. ID 211605); published September 5, 2014

We propose and analyze a novel all-optical fiber polarization scrambler based on the transfer (via the Kerr effect) of the intensity fluctuations of an incoherent pump beam into polarization fluctuations of a frequency-shifted signal beam, copropagating in a randomly birefringent telecom fiber. Optimal signal polarization scrambling results whenever the input signal and pump beams have nearly orthogonal states of polarization. The nonlinear polarization scrambler may operate on either cw or high-bit-rate pulsed signals. © 2014 Optical Society of America

OCIS codes: (060.4370) Nonlinear optics, fibers; (060.2340) Fiber optics components; (190.3270) Kerr effect; (060.7140) Ultrafast processes in fibers; (060.4510) Optical communications.
http://dx.doi.org/10.1364/OL.39.005309

The capability to control the state of polarization (SOP) of light is of vital importance in a host of applications, ranging from optical communications to lasers and sensing and imaging technologies. In the context of fiber optic communication systems, it is often necessary to achieve ultrafast SOP control, which has been traditionally enabled by using waveguide electro-optic phase modulation techniques [1] or fiber squeezers [2]. The input polarization scrambling of telecom signals is extensively used in light-wave communications [3]. For example, signal depolarization within a forward error correction frame permits the washing out of polarization mode dispersion (PMD)-induced error bursts [4,5]. Signal polarization scrambling also reduces noise accumulation from polarization dependent gain in erbium-doped amplifiers [6]. Moreover, bit-synchronous polarization scrambling of on–off keying signals also introduces a signal phase modulation that mitigates nonlinear impairments [7].

The operating speed of existing polarization scramblers is limited by modulator driving electronics. When aiming at 100 GHz depolarization speeds or higher, it is thus of fundamental interest to conceive a depolarizer based on the virtually instantaneous Kerr nonlinear response of fibers. In this Letter, we propose and numerically demonstrate the proof-of-principle operation of a Kerr-based ultrafast depolarizer. Thanks to Kerr cross-polarization modulation, we show that it is possible to efficiently convert the intensity fluctuations of an incoherent pump wave into polarization fluctuations of a frequency-detuned, constant-intensity signal beam. The proposed device is based on the same physical principles that have recently permitted the demonstration of the ultrafast repolarization of an initially depolarized signal through the polarization attraction effect [8,9].

Let us consider the evolution in a telecom fiber with random birefringence of a polarized light field with envelope $\mathbf{E}(z,t) = [E_x(z,t), E_y(z,t)]$. We assume we are operating in the so-called Manakov limit, which applies for a propagation distance $L \ll L_d$, where L_d is the PMD diffusion length. In this case, wave propagation is described by the coupled nonlinear Schrödinger (CNLS) equations [10]

$$\partial_z E_a + i\frac{\beta_2}{2}\partial_{tt}E_a = i\frac{8\gamma}{9}(|E_a|^2 + |E_b|^2)E_a - \alpha E_a, \qquad (1)$$

where $\{a,b\} = \{x,y\}$, $a \neq b$, and γ is the scalar nonlinear coefficient of the fiber; β_2 is the group-velocity dispersion (GVD) coefficient at a reference frequency (say, ω_r); and α is the linear loss coefficient. Let us consider first the following approximations in Eq. (1), which permit an analytical description of the polarization scrambler. We set $\mathbf{E}(z,t) = \mathbf{E}_p(z,t) + \mathbf{E}_s(z,t)$, where $\mathbf{E}_p$ and $\mathbf{E}_s$ are pump and signal beams at frequencies $\omega_p = \omega_r - \omega$ and $\omega_s = \omega_r + \omega$, respectively. By supposing that temporal variations of both pump and signal waves are sufficiently slow, so that intrachannel GVD effects may be neglected, and for relatively short fibers so that we may set $\alpha = 0$, Eq. (1) may be conveniently expressed in terms of the dimensionless Stokes vectors of the pump $\mathbf{P} = [P_1, P_2, P_3]$ and signal $\mathbf{S} = [S_1, S_2, S_3]$ as [10]

$$\partial_\xi \mathbf{P} \mp \delta\partial_\tau \mathbf{P} = \frac{8}{9}\mathbf{S}\times\mathbf{P}; \qquad \partial_\xi \mathbf{S} \pm \delta\partial_\tau \mathbf{S} = \frac{8}{9}\mathbf{P}\times\mathbf{S}. \qquad (2)$$

Here, we introduce the dimensionless propagation distance $\xi \equiv z/L_{\mathrm{NL}}$, where $L_{\mathrm{NL}}^{-1} = \gamma\langle S_0\rangle$ and $\langle S_0\rangle$ is the signal average power, and time $\tau = t/T_{\mathrm{NL}}$, where $T_{\mathrm{NL}} = (|\beta_2|L_{\mathrm{NL}}/2)^{1/2}$, respectively. The brackets $\langle\rangle$ denote temporal averaging. Moreover, in Eq. (2), upper and lower signs hold for anomalous or normal GVD, respectively, and $\delta = 2\omega T_{\mathrm{NL}}$ denotes the group-velocity mismatch (GVM) between pump and signal, which are centered at the normalized frequencies $\mp\delta/2$, respectively.

Pump and signal average powers $\langle P_0\rangle = \langle|\mathbf{P}|\rangle$ and $\langle S_0\rangle = \langle|\mathbf{S}|\rangle$ remain constant upon propagation. Thus, we may set $\langle S_0\rangle = 1$. Moreover, the GVM simply leads to a temporal translation of the power profiles with distance—namely, $P_0(\xi,\tau) = P_0(0, \tau \pm \delta\xi)$ and $S_0(\xi,\tau) = S_0(0, \tau \mp \delta\xi)$. Similarly, the time average $\langle\mathbf{\Omega}\rangle$ of the pivot vector $\mathbf{\Omega} = \mathbf{S} + \mathbf{P}$ is a conserved quantity of Eq. (2). The analytical solution of Eq. (2) in the cw limit is [11]

$$\mathbf{V} = \mathbf{b_{1v}} + \mathbf{b_{2v}}\cos(|\mathbf{\Omega}|\xi) + \mathbf{b_{3v}}\sin(|\mathbf{\Omega}|\xi), \quad (3)$$

where $\mathbf{V} = \{\mathbf{P}, \mathbf{S}\}$, $\mathbf{b_{1v}} = (\mathbf{\Omega}\cdot\mathbf{V}(0)/|\mathbf{\Omega}|^2)\mathbf{\Omega}$, $\mathbf{b_{2v}} = \mathbf{V}(0) - \mathbf{b_{1v}}$, and $\mathbf{b_{3v}} = (\mathbf{\Omega}\times\mathbf{V}(0)/|\mathbf{\Omega}|)$. Hence, $\mathbf{P}(z)$ and $\mathbf{S}(z)$ rotate about the constant and known pivot $\mathbf{\Omega}$.

Now, we relax the cw hypothesis by allowing the input Stokes vectors $\mathbf{P}(0,\tau)$ and $\mathbf{S}(0,\tau)$ to vary in time. In this case, one may still solve Eq. (2) by the standard split-step procedure: at each position ξ, we advance over a spatial step h by first analytically computing the nonlinear evolution from ξ to $\xi + h$ from Eq. (3). Next, the action of the GVM is evaluated by applying opposite linear temporal shifts $\pm\delta h$ to the Stokes vectors of the signal and pump.

Let us now consider the copropagation of a signal with constant power—namely, $S_0(\xi,\tau) = S_0(0,\tau - \delta\xi) = 1$ and a pump with a time-varying Stokes vector $\mathbf{P}(\xi,\tau)$. The nonlinear step of the evolution of $\mathbf{S}$ from ξ to $\xi + h$ at two points in time (say, τ_1 and τ_2) is obtained as a precession on the unitary Poincaré sphere around the different local pivots $\mathbf{\Omega}(\xi,\tau_{1,2}) = \mathbf{S}(\xi,\tau_{1,2}) + \mathbf{P}(\xi,\tau_{1,2})$. Thus, one may expect that, in general, an initially fully polarized signal field may become gradually depolarized upon propagation through its cross-polarization interaction with a time-varying pump beam.

For a cw signal that copropagates with a partially coherent pump beam whose instantaneous power exhibits random temporal fluctuations (refer to Fig. 1), the initially unitary degree of polarization (DOP) of the signal is progressively reduced along the fiber as a result of pump-induced nonlinear SOP scrambling.

Ideal scrambling (i.e., a signal DOP = 0) could be obtained if the pump power values at any position along the fiber were fully uncorrelated in time so that the two corresponding precessions of the signal Stokes vector are also uncorrelated. In such a situation, after a certain propagation distance, the temporal evolution of the signal Stokes vector would trace a random path on the Poincaré sphere. In practice, nearly ideal scrambling may still be achieved by using an *incoherent pump* beam with finite but short correlation time, e.g., using filtered amplified spontaneous emission (ASE) noise.

We simulated the depolarized pump source provided by filtered ASE noise by independently generating its polarization components $E_{px}(0,\tau)$ and $E_{py}(0,\tau)$ through bandpass filtering a white noise field, obtained by adding

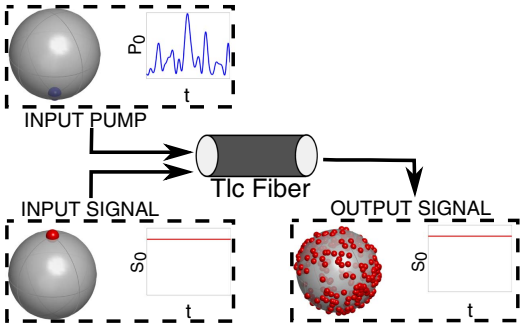

Fig. 1. Schematic of a nonlinear SOP scrambler: fully polarized incoherent pump (black and blue online) and orthogonal cw signal (gray and red online) are injected in a randomly birefringent fiber. Temporal fluctuations of the input pump power P_0 lead to a depolarized signal; signal power is unaffected.

at each frequency sample a random variable with independent Gaussian-distributed real and imaginary components. We used a Gaussian filter transfer function of the form $H(\nu) = \exp[-(\nu + \delta/2)^2]/(2\sigma_p^2)$, where ν is the normalized frequency, whereas for simulating a fully polarized input pump, we simply set $E_{py}(0,\tau) = C\cdot E_{px}(0,\tau)$, being $C \in \mathbb{C}$. The degree of pump temporal coherence is measured by the input coherence time $\tau_{\mathrm{coh},p}(0)$, where $\tau_{\mathrm{coh},v}(\xi) = \int_{\tau'}(|\langle E_{va}(\xi,\tau)E_{va}(\xi,\tau+\tau')^*\rangle|/\langle|E_{va}(\xi,\tau)|^2\rangle)^2\partial\tau'$ $(a = \{x,y\}, v = \{p,s\})$.

In order to evaluate the effectiveness of the nonlinear depolarization process depicted in Fig. 1, we computed the evolution with distance of the signal $\mathrm{DOP}(\xi) = |\langle\mathbf{S}\rangle| = (\langle S_1(\xi,\tau)\rangle^2 + \langle S_2(\xi,\tau)\rangle^2 + \langle S_3(\xi,\tau)\rangle^2)^{1/2}$. The DOP does not provide any information about the time scale of the temporal fluctuations of $\mathbf{S}(\xi,\tau)$ at any given position ξ along the fiber. Clearly, the faster the temporal fluctuations of $\mathbf{S}(\xi,\tau)$, the shorter the temporal duration of the input pump burst that is needed for efficient signal depolarization. To quantify the scrambling speed, we introduce the quantity $s_{\mathrm{scr}}(\xi) = \langle|\partial\mathbf{S}(\xi,\tau)/\partial\tau|\rangle$, which measures the average angular rotation speed of the temporal trajectory of the signal Stokes vector.

Because of the symmetry of Eq. (2), the spatiotemporal evolution of $\mathbf{P}(\xi,\tau)$ and $\mathbf{S}(\xi,\tau)$ only depends on the angle—say, $\beta(\tau)$ between $\mathbf{P}(0,\tau)$ and $\mathbf{S}(0,\tau)$ at the fiber entry [11]. With no loss of generality, we may limit ourselves to consider an input cw signal that is fully polarized along the x axis so that $\mathbf{S}(0,\tau) = \mathbf{S}(0) = [0,0,1]$.

The conservation of $\langle\mathbf{\Omega}\rangle$ imposes that the signal $\mathrm{DOP} = |\langle\mathbf{S}\rangle| = |\langle\mathbf{\Omega}\rangle - \langle\mathbf{P}\rangle|$; thus, $|\langle\mathbf{\Omega}\rangle| = |\langle\mathbf{P}\rangle|$ is a necessary condition in order to achieve a full signal depolarization (i.e., DOP = 0). Whenever the input pump is also fully polarized, the input relative angle between the Stokes vectors of the pump and the signal is independent of time, i.e., $\beta(\tau) = \beta$ and $\langle P_0\rangle = \max\{|\langle\mathbf{P}\rangle|\}$. Thus, the condition $|\langle\mathbf{\Omega}\rangle| = |\langle\mathbf{P}\rangle|$ implies that $|\langle\mathbf{\Omega}\rangle| \le \langle P_0\rangle$.

Because $|\langle\mathbf{\Omega}\rangle|^2 = \langle P_0\rangle^2 + \langle S_0\rangle^2 + 2\langle P_0\rangle\langle S_0\rangle\cos(\beta)$ and $\langle S_0\rangle = 1$, the condition $|\langle\mathbf{\Omega}\rangle| \le \langle P_0\rangle$ means that $\beta_c \le \beta \le \pi$, where $\beta_c = \arccos[-(2\langle P_0\rangle)^{-1}]$. Therefore, for achieving complete signal depolarization at the fiber output, the input angle between the pump and signal Stokes vectors must be larger than the critical value β_c.

A better estimate of β_c, although not rigorous, may be based on the fact that the pump and signal Stokes vectors experience a symmetric evolution around the randomly varying local pivots $\mathbf{\Omega}(\xi,\tau)$; we thus expect that, after a sufficiently long propagation distance, the degree of depolarization of the pump should be comparable to that of the signal.

Our numerical simulations confirm this assumption, which leads to the empirical relation $|\langle\mathbf{P}(\xi,\tau)\rangle| - \langle P_0\rangle \approx |\langle\mathbf{S}(\xi,\tau)\rangle| - \langle S_0\rangle$. Therefore, the equality $|\langle\mathbf{\Omega}\rangle| = |\langle\mathbf{P}\rangle|$ can be rewritten as $|\langle\mathbf{\Omega}\rangle| = \langle P_0\rangle + |\langle\mathbf{S}(\xi,\tau)\rangle| - \langle S_0\rangle$. Accordingly, in order to obtain a signal $\mathrm{DOP} = |\langle\mathbf{S}(\xi,\tau)\rangle| = 0$, the pump power $\langle P_0\rangle$ should be at least as large as the signal power $\langle S_0\rangle$, and the input pump and signal Stokes vectors should be antiparallel ($\beta_c \to \pi$). The previous estimations of β_c do not vary when propagation losses are taken into account.

As a matter of fact, for either parallel or antiparallel input pump and signal Stokes vectors, the input SOP and DOP of both beams remain, in principle, unchanged

in propagation, as Eq. (2) leads to $\mathbf{P}(\xi,\tau)=\mathbf{P}(0,\tau\pm\delta\xi)$ and $\mathbf{S}(\xi,\tau)=\mathbf{S}(0,\tau\mp\delta\xi)=[0,0,1]$ in both cases. Yet in the antiparallel case, the fixed point solutions of Eq. (2) are unstable with respect to small perturbations. Therefore, in the presence of weak input background ASE noise, one obtains an effective diffusion of the signal Stokes vector $\mathbf{S}$ over the entire Poincaré sphere, which ultimately leads to the most efficient configuration for scrambling the signal SOP (refer to Figs. 1 and 2). Clearly, even if $\mathbf{S}(0,\tau)$ and $\mathbf{P}(0,\tau)$ are antiparallel, the Stokes vectors of the depolarized signal and pump noise components—say, $\eta_p(0,\tau)$ and $\eta_s(0,\tau)$—generate instantaneous input Stokes vectors $\mathbf{S}(0,\tau)+\eta_s(0,\tau)$ and $\mathbf{P}(0,\tau)+\eta_p(0,\tau)$ that are no longer strictly antiparallel.

Whenever the input incoherent pump is almost fully depolarized so that $\langle\mathbf{P}(0,\tau)\rangle\approx[0,0,0]$, its depolarization will be preserved upon propagation. More precisely, for a cw input depolarized pump, i.e., with a temporally constant magnitude of the Stokes vector, one observes its repolarization toward the input signal SOP [11]. However, random temporal fluctuations of the intensity of the incoherent pump compromise such a possibility. Consequently, at each position ξ along the fiber, one has $\langle\mathbf{P}(\xi,\tau)\rangle\approx[0,0,0]$; moreover, the conservation of $\langle\mathbf{\Omega}\rangle$ implies that $\langle\mathbf{S}(\xi,\tau)\rangle\approx[0,0,1]$, i.e., the signal remains nearly fully polarized upon propagation (Fig. 2).

Let us now present some examples of the numerical resolution of Eq. (1) in order to validate our analytical predictions. Consider the nonlinear evolution along the fiber of an input cw signal along with an incoherent pump with $\langle P_0\rangle=1.5$. In order to avoid a significant nonlinear spectral broadening of the pump, which may even lead to its overlap with the signal band, a sufficiently large intraband dispersion should be introduced within the pump bandwidth. According to [12], the intraband dispersion length of the pump, which in normalized units reads as $L_D=\tau_{\mathrm{coh},p}^2$, should be no more than a few nonlinear lengths. We thus set $\tau_{\mathrm{coh},p}\approx 1$. The pump-signal GVM was set to $\delta=3$, and propagation losses were set to $\alpha=0$.

In Fig. 2, we analyze different configurations involving a linearly polarized input pump with $\beta=\{\pi/2,0.94\pi,\pi\}$. We also consider the case of a depolarized input pump. We numerically solved the full model Eq. (1) and filtered the output spectra around their respective central frequencies in order to detect the signal and pump fields $E_{sx,sy}(\xi,\tau)$ and $E_{px,py}(\xi,\tau)$. A background wideband noise was applied with an optical pump-to-noise power ratio in the pump band of 67 dB.

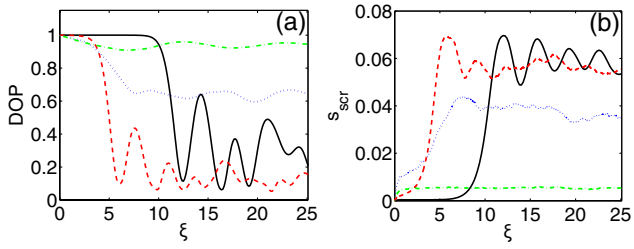

Fig. 2. Different relative pump-signal polarization configurations (see text for details). (a) Signal degree of polarization (DOP). (b) Scrambling speed. Antiparallel case $\beta=\pi$ (black solid line); $\beta=0.94\pi$ (red-dashed line); $\beta=\pi/2$ (blue-dotted line); depolarized pump (green-dashed line). In order to express the scrambling speeds in rad/s, the values in (b) should be normalized with respect to the nonlinear time T_{NL}.

For each configuration, the computed evolution with distance of the DOP and the scrambling speed of the signal are shown in Fig. 2. As expected, a depolarized input pump does not provide effective signal SOP scrambling. To the contrary, whenever the input pump is orthogonally polarized with respect to the input signal (i.e., their Stokes vectors are antiparallel), one obtains a strong signal depolarization. In this case, the signal DOP reaches a first minimum of approximately 0.1 at the distance $\xi\approx 12$.

It can also be seen in Fig. 2 that the antiparallel case, even though it ultimately leads to efficient scrambling, is also characterized by the lowest scrambling speed in the first stages of the signal propagation. In fact, as previously discussed, Eq. (2) predicts that in the absence of a background depolarized noise, the signal scrambling speed would remain strictly equal to zero so that no scrambling results. However, input noise leads to a weakly depolarized signal, whose SOP slowly moves (i.e., with an initial scrambling speed close to zero) away from the antiparallel condition.

For increasing the initial scrambling speed, thus decreasing the fiber length at which effective depolarization is first observed, it proves useful to slightly reduce below π the input relative angle β. Figure 2 shows that, whenever $\beta=0.94\pi$, one reduces down to $\xi\approx 6$ the position of the first minimum of the signal DOP. Figure 2 also shows that a too-strong reduction of the input angle β leads to a significant drop of the scrambling efficiency, e.g., for $\beta=\pi/2$, the signal DOP remains above 0.6 at all distances.

Note in Fig. 2 that, for $\beta=0.94\pi$ and $\beta=\pi$, the first minimum of the DOP is followed by some oscillations, indicating a sequence of partial repolarizations and depolarizations of the signal, whereas for $\xi>25$ the signal DOP remains below 0.2, corresponding to an effective scrambling over the Poincaré sphere. The spatial evolution of the DOP oscillations strictly depends on the particular realization of the input random background noise and incoherent pump. In fact, the oscillations disappear if the evolution of the signal DOP is averaged over a number of independent random noise and pump realizations.

Figure 3(a) shows the average DOP over 50 such realizations, where $\langle P_0\rangle$ is randomly chosen between 1.5 and 2, δ is between 2 and 4, $\tau_{\mathrm{coh},p}(0)$ is between 0.5 and 2, and β is between 0.89π and π. Although the DOP oscillations are largely washed out in Fig. 3(a), one still obtains a minimum of the average DOP at $\xi\approx 6$. The reason is that, for this range of parameters, a minimum of the DOP is always observed near $\xi=6$ for each individual noise and pump realization. A typical distribution of the output tips of the signal Stokes vector $\mathbf{S}(\xi=6,\tau)$ on the Poincaré sphere is shown in the inset of Fig. 3(a), demonstrating the occurrence of effective signal SOP scrambling over the entire sphere.

Although the average pump and signal powers, $\langle P_0\rangle$ and $\langle S_0\rangle$, are truly conserved, Fig. 3(b) shows that the output temporal profile $S_0(\xi=6,\tau)$, which results from the numerical solution of Eq. (1), exhibits weak and relatively short-scale fluctuations. We point out that the numerical solution of Eq. (2) provides the same

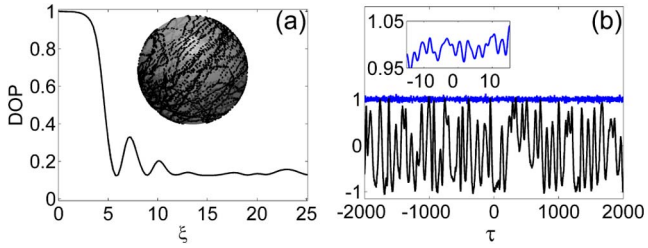

Fig. 3. (a) Average signal degree of polarization (DOP) over 50 random realizations (see text for details) and output distribution of the signal $\mathbf{S}(\xi = 6, \tau)$ over the Poincaré sphere (inset). (b) $S_0(\xi = 6, \tau)$ (blue) and $S_1(\xi = 6, \tau)$ (black); inset shows a temporal zoom of the fast fluctuations of S_0. Plots in (b) and sphere in (a) refer to a particular yet typical random realization.

DOP and scrambling speeds shown in Figs. 2 and 3, but it does not capture such power fluctuations. We thus ascribe these fluctuations to the interplay of intraband dispersion and cross-phase modulation. Figure 3(b) shows the output temporal profile $S_0(\xi = 6, \tau)$ for a selected realization of the combined random noise and incoherent pump. Although, in this case, the fluctuations are bound in the narrow range (0.95–1.05), they may be considerably enhanced when increasing the mean pump power $\langle P_0 \rangle$. This places an upper bound to the admissible pump power.

Because of the pump-signal GVM δ, the signal does not respond to the instantaneous pump variations but, rather, to their average over a time window that grows larger with δ. Therefore, a reduction of the parasitic signal power fluctuations can be simply achieved by increasing the pump-signal frequency shift.

In addition to the parasitic signal power fluctuations, the speed s_{scr} also grows larger with $\langle P_0 \rangle / \delta$. In fact, the larger the pump power and its associated fluctuations, the faster the signal scrambling speed. However, the speed may be reduced by increasing the signal-pump frequency detuning, which leads to an effective averaging of the pump power fluctuations.

Because of the resulting nonlocal nonlinear response, generally, the coherence time of the output signal is far greater than that of the input pump. For example, at $\xi = 6$, the average value over the 50 realizations of the signal coherence (or depolarization) time is $\tau_{\mathrm{coh},s}(\xi = 6) \approx 75$. This aspect opens up two interesting depolarization scenarios for a fiber of length L, which are tied to the output coherence time $\tau_{\mathrm{coh},s\text{–cw}}(\xi = L)$ of a cw signal that is affected by the depolarization process. First, it is possible to depolarize even a fully polarized input signal pulse of width T, provided that $T \gg \tau_{\mathrm{coh},s\text{–cw}}(\xi = L)$. Second, if a sufficiently long train of fully copolarized signal pulses with width $T \ll \tau_{\mathrm{coh},s\text{–cw}}(\xi = L)$ is injected at the input, the entire signal pulse train can still be efficiently depolarized while preserving a nearly constant SOP within each individual pulse. Actually, the output DOP of the whole signal may be reduced to zero, while the DOP calculated for any individual pulse remains close to unity.

In real units, for $\langle S_0 \rangle = 1$ W, $\gamma = 1\ \mathrm{W^{-1}\,km^{-1}}$, and a GVD of 20.4 $\mathrm{ps^2\,km^{-1}}$ ($D = -16\ \mathrm{ps\,nm^{-1}\,km^{-1}}$ at 1550 nm), one obtains $L_{\mathrm{NL}} = 1$ km and $T_{\mathrm{NL}} \approx 3.2$ ps. Moreover, the detuning between the pump and signal is 1.2 nm, so that for a PMD coefficient $D_p < 0.25\ \mathrm{ps\,km^{-1/2}}$, one has $L_d > 55\ \mathrm{km} \gg L$ [10]. The device bandwidth is mainly limited by PMD: with $D_p = 0.06\ \mathrm{ps\,km^{-1/2}}$, a detuning up to 5 nm is possible. Thus, a few kilometers of standard single-mode fiber are sufficient to achieve effective signal depolarization. The corresponding typical temporal duration of the output signal SOP fluctuations will be of the order of 200 ps and the scrambling speed of approximately 20 Grad/s (Fig. 3). When introducing small propagation losses α of approximately 0.2 dB/km, all the main results discussed in our work do not change.

In conclusion, we proposed and demonstrated the proof-of-principle concept of a novel all-optical and ultrafast SOP scrambler based on the nonlinear copropagation and Kerr–nonlinearity mediated interaction of a signal and an incoherent pump beam in a randomly birefringent telecom fiber. Whenever the input signal and pump beams have nearly orthogonal SOPs, the fast temporal oscillations of the pump power lead to an effective SOP scrambling of the signal. At the same time, the signal power remains virtually unchanged. The nonlinear depolarizer may operate on either cw or pulsed signals and on high-bit-rate ultrashort pulse trains.

This research was funded by the European Research Council under Grant Agreement 306633, ERC PETAL, the iXCore Foundation, and the Italian Ministry of University and Research (MIUR) (Grant Contract 2012BFNWZ2).

References

1. F. Heismann, D. A. Gray, B. H. Lee, and R. W. Smith, IEEE Photon. Technol. Lett. **6**, 1156 (1994).
2. L. Yao, H. Huang, J. Chen, E. Tan, and A. Willner, Opt. Express **20**, 1691 (2012).
3. P. K. J. Park, J. H. Lee, and Y. C. Chung, Opt. Eng. **47**, 035005 (2008).
4. B. Wedding and C. N. Haslach, "Enhanced PMD mitigation by polarization scrambling and forward error correction," in *Proceedings of Optical Fiber Communication Conference*, Anaheim, CA, USA, 2001, paper WAA1.
5. Z. Li, J. Mo, Y. Wang, and C. Lu, "Experimental evaluation of the effect of polarization scrambling speed on the performance of PMD mitigation using FEC," in *Proceedings of Optical Fiber Communication Conference*, Los Angeles, CA, USA, 2004, paper MF69.
6. N. S. Bergano, V. J. Mazurczyk, and C. R. Davidson, "Polarization scrambling improves SNR performance in a chain of EDFAs," in *Proceedings of Optical Fiber Communication Conference*, San José, CA, USA, 1994, paper ThR4.
7. N. S. Bergano and C. R. Davidson, J. Lightwave Technol. **14**, 1299 (1996).
8. P. Morin, J. Fatome, C. Finot, S. Pitois, R. Claveau, and G. Millot, Opt. Express **19**, 17158 (2011).
9. J. Fatome, S. Pitois, P. Morin, E. Assemat, D. Sugny, A. Picozzi, H. R. Jauslin, G. Millot, V. V. Kozlov, and S. Wabnitz, Sci. Rep. **2**, 938 (2012).
10. V. V. Kozlov, M. Barozzi, A. Vannucci, and S. Wabnitz, J. Opt. Soc. Am. B **30**, 530 (2013).
11. V. V. Kozlov, K. Turitsyn, and S. Wabnitz, Opt. Lett. **36**, 4050 (2011).
12. A. Picozzi, Opt. Express **15**, 9063 (2007).